

This is the final peer-reviewed accepted manuscript of:

Preferential nitrite inhibition of the mitochondrial F1FO-ATPase activities when activated by Ca(2+) in replacement of the natural cofactor Mg(2+).

Nesci S, Ventrella V, Trombetti F, Pirini M, Pagliarani A. Biochim Biophys Acta. 2016 Feb;1860(2):345-53.

The final published version is available online at:
<https://doi.org/10.1016/j.bbagen.2015.11.004>

Rights / License:

The terms and conditions for the reuse of this version of the manuscript are specified in the publishing policy. For all terms of use and more information see the publisher's website.

This item was downloaded from IRIS Università di Bologna (<https://cris.unibo.it/>)

When citing, please refer to the published version.

Preferential nitrite inhibition of the mitochondrial F_1F_0 -ATPase activities when activated by Ca^{2+} in replacement of the natural cofactor Mg^{2+} : new insights in the cardio-protection by nitrite?

Salvatore Nesci, Vittoria Ventrella, Fabiana Trombetti, Maurizio Pirini,
Alessandra Pagliarani

Department of Veterinary Medical Sciences (DIMEVET), University of Bologna, via Tolara di Sopra 50, 40064 Ozzano Emilia (BO)

Corresponding author: Alessandra Pagliarani, alessandra.pagliarani@unibo.it Tel 0039 051 2097017, fax 0039 051 2097017

Keywords: Mitochondria; F_1F_0 -ATPase; nitrite; post-translational modifications; calcium; dityrosine.

Abbreviations: ASC, ascorbate; BHQ, 2,5-Di-*tert*-butylhydroquinone; Ca-ATPase(s), Ca^{2+} -activated F_1F_0 -ATPase; CsA, cyclosporin A; DMSO, dimethylsulfoxide; DTT, DL-Dithiothreitol; GSH, reduced glutathione; H_2O_2 , hydrogen peroxide; IMM, inner mitochondrial membrane; I/R, ischemia/reperfusion; Mg-ATPase(s), Mg^{2+} -activated F_1F_0 -ATPase; MPT, mitochondrial permeability transition; MPTP, mitochondrial permeability transition pore; $\cdot NO$, nitric oxide; NO_2^- , nitrite; $\cdot NO_2$, nitrogen dioxide radical; PTIO, 2-Phenyl-4,4,5,5-tetramethylimidazoline-1-oxyl 3-oxide; ROS, reactive oxygen species; TOC, (\pm)- α -Tocopherol.

Abstract

Background

The mitochondrial F_1F_0 -ATP synthase has not only the known life function in building most cellular ATP, but also, as recently hinted, an amazing involvement in cell death. Accordingly, the two-faced enzyme complex, which catalyzes both ATP synthesis and ATP hydrolysis, has been involved in the mitochondrial permeability transition, the master player in apoptosis and necrosis. Nitrite, a cellular nitric oxide reservoir, has a recognized role in cardiovascular protection, through still unclear mechanisms.

Methods

In swine heart mitochondria the effect of nitrite on the F_1F_0 -ATPase activity activated by Ca^{2+} , henceforth defined as Ca-ATPase(s) or by the natural cofactor Mg^{2+} , was investigated by evaluating ATP hydrolysis under different assay conditions.

Results

Ca^{2+} is far less efficient than the natural cofactor Mg^{2+} in the ATPase activation. However, when activated by Ca^{2+} the ATPase activity is especially responsive to nitrite, which acts as uncompetitive inhibitor and up to 2 mM inhibits the Ca^{2+} -activated-ATPase(s), probably by promoting dytyrosine formation on the enzyme proteins, leaving the Mg -ATPase(s) unaffected. Most likely these ATPases refer to the same F_1F_0 complex, even if coexistent ATPases may overlap.

Conclusions

The preferential inhibition by nitrite of the Ca-ATPase(s), due to post-translational tyrosine modifications, may prevent the calcium-dependent functionality of the mitochondrial F_1F_0 complex and related events.

General significance

The ATPase inhibition by nitrite under Ca^{2+} overload in mitochondria may contribute to the nitrite cardio-protective properties. Nitrite would quench ATP hydrolysis and the negative events linked to the calcium-dependent functioning mode of the F_1F_0 complex under ischemia/reperfusion conditions.

1. Introduction

The mammalian mitochondrial F_1F_0 -ATPase (EC 3.6.3.14) is a membrane-bound protein complex of ~600-kDa including the rotary catalytic motor F_1 and a membrane turbine (ion pump) motor F_0 , connected by a central and a peripheral stalk [1,2]. The F_1F_0 -ATPase is the master enzyme for massive ATP production by oxidative phosphorylation. Accordingly, the F_1F_0 complex dissipates the protonmotive force (Δp) produced by the oxidation of nutrient substrates in mitochondrial respiration to produce ATP. The peculiar ability of the F_1F_0 -ATPase turbine to operate also in reverse allows ATP hydrolysis and the rebuilding of the membrane potential under pathophysiological conditions which depolarize the inner mitochondrial membrane (IMM) [3]. The two opposite ATP synthesis/hydrolysis functions of the hydrophilic domain F_1 are coupled to ion translocation across the membrane by the transmembrane F_0 sector. This coupling is ensured by a torque generation mechanism [4] with sustains two opposite rotation directions [5]. The enzyme complex, which over time has fascinated many scientists for its marvelous molecular mechanism, has recently lead to envisage its mysterious involvement in cell death [6,7]. The tight regulation of IMM permeability to substrates, cations, especially H^+ , is crucial for ATP production. Cellular events leading to uncontrolled regulation of calcium translocation in the mitochondrial matrix accompanied by exacerbated reactive oxygen species (ROS) formation, high P_i concentration and adenine nucleotide depletion, cause a Δp drop leading to the Mitochondrial Permeability Transition (MPT). In turn MPT is linked to osmotic shifts, mitochondrial dysfunctions and eventually cell death. The molecular identity triggering MPT is the so-called Mitochondrial Permeability Transition Pore (MPTP), of still unknown nature, but in which the F_1F_0 -complex has been repeatedly involved [8-11]. MPT and mitochondrial dysfunction play a crucial role in the progression of ischemia/reperfusion (I/R) injury, which accompanies several diseases that cause morbidity and mortality [12,13] in Western countries. Mitochondrial respiration in ischemic tissues is inhibited by oxygen lack, resulting in ATP deficiency [3]. Upon oxygen reintroduction, *i.e.* reperfusion, the electron-deficient molecular species accumulated within the respiratory chain during ischemia lead to oxidative stress. Then, prolonged oxidative stress and Ca^{2+} massive influx in mitochondria trigger MPT [13].

Recently, nitrite (NO_2^-), a naturally occurring inorganic anion, was shown to modulate the mitochondrial function, mediate cytoprotection after I/R and to be implicated in highly protective ischemic preconditioning program signaling [12,14]. However the mechanisms involved in the nitrite-mediated cytoprotection are still unclear. Several mitochondrial proteins are known to be

affected by nitrite and MPT inhibition by nitrite has been ascribed to the inhibition of respiratory complexes [15].

One of the most common sources of nitrite is the reduction of nitrate, greedily uptaken by green leafy vegetables and beetroot [15,16]. Thus, through the entero-salivary circuit, these plants provide mammals with a precious source of nitrite. In turn, nitrite constitutes a bioavailable endocrine reservoir supporting nitric oxide (NO) signalling during metabolic stress as ischemia and acidosis, being bioactivated by both enzymatic and non-enzymatic reactions [15,17]. Increasing evidence points out the nitrate-nitrite-NO pathway as candidate regulator of the cardiovascular system [18]. Recently, dietary nitrite and nitrate supplementation emerges as promising nutritional therapy to reduce risks of cardiovascular disease, myocardial infarction, and stroke [19]. The beneficial health effects may be achievable at intake levels resulting from the daily consumption of nitrate-rich vegetables [20] and have a therapeutic potential at high micromolar doses [19].

In this paper, we provide evidence shouldering a putative control mechanism exerted by nitrite on the mitochondrial F_1F_0 -ATPase activity when the enzyme activity is stimulated by Ca^{2+} in the absence of Mg^{2+} . The findings may contribute to enlighten the mechanisms of nitrite involvement in cytoprotection.

2. Material and methods

2.1. Chemicals

Na_2ATP , oligomycin mixture (A:B:C 64:15:17%), L-glutathione reduced form (GSH), L-Ascorbic acid (ASC), 2,5-Di-*tert*-butylhydroquinone (BHQ), hydrogen peroxide solution (H_2O_2), DL-Dithiothreitol (DTT), (\pm)- α -Tocopherol (TOC), sodium orthovanadate and sodium nitrite ($NaNO_2$) were obtained from Sigma–Aldrich (Milan, Italy). Cyclosporin A (CsA), 2-Phenyl-4,4,5,5-tetramethylimidazoline-1-oxyl 3-oxide (PTIO) and sodium nitrate ($NaNO_3$) were purchased by Vinci-Biochem (Vinci, Italy). All other chemicals were reagent grade. Quartz double distilled water was used for all reagent solutions except when differently stated.

2.2. Preparation of the mitochondrial fraction

Swine hearts (*Sus scrofa domesticus*) were collected at a local abattoir and transported to the lab within 2 h in ice buckets at 0-4°C. After removal of fat and blood clots as much as possible, approximately 30-40 g of heart tissue were rinsed in ice-cold washing Tris-HCl buffer (medium A) consisting of 0.25 M sucrose, 10 mM Tris(hydroxymethyl)-aminomethane (Tris), pH 7.4 and finely chopped into fine pieces with scissors. Each preparation was made from one heart. Once rinsed,

tissues were gently dried on blotting paper and weighted. Then tissues were homogenized in the homogenizing buffer (medium B) consisting of 0.25 mM sucrose, 10 mM Tris, 0.2 mM EDTA (free acid), 0.5 mg/mL BSA, pH 7.4 with HCl. After a preliminary gentle break up by Ultraturrax T25, the tissue was carefully homogenized by a motor-driven teflon pestle homogenizer (Braun Melsungen Type 853202) at 650 rpm with 3 up-and-down strokes. The mitochondrial fraction was then obtained by stepwise centrifugation (Sorvall RC2-B, rotor SS34) [21]. Briefly, the homogenate was centrifuged at 1,000 g for 5 min, thus yielding a supernatant and a pellet. The pellet was re-homogenized under the same conditions of the first homogenization and re-centrifuged at 1,000 g for 5 min. The gathered supernatants from these two centrifugations, filtered through four cotton gauze layers, were centrifuged at 10,500 g for 10 min to yield the raw mitochondrial pellet. The raw pellet was resuspended in medium A and further centrifuged at 10,500 g for 10 min to obtain the final mitochondrial pellet. The latter was resuspended by gentle stirring using a Teflon Potter Elvehjem homogenizer in a small volume of medium A, thus obtaining a protein concentration of 20-25 mg/mL. All steps were carried out at 0-4 °C. The protein concentration was determined according to the colorimetric method of Bradford [22] by Bio-Rad Protein Assay kit II with bovine serum albumin (BSA) as standard. The mitochondrial preparations were then stored in liquid nitrogen until the evaluation of ATPase activities.

2.3. Preincubation and treatment of mitochondria

When combined effects of different effectors were tested, to ensure interaction of these compounds with mitochondrial proteins, mitochondria were preincubated for 30 min in ice [23] with appropriate concentrations of nitrite and/or other effectors immediately prior to further analyses. In these experiments the preincubation system (50 μ L) contained 40 μ L mitochondrial suspensions plus 10 μ L of medium A (control), or 10 μ L of appropriate nitrite solutions in medium A to yield the desired final concentrations to be tested in the reaction system.

To evaluate the formation of *S*-nitrosylation products, the nitrite-preincubated mitochondrial suspensions were treated with the reducing agent ascorbate (ASC) and/or with GSH, to check any possible transnitrosation reaction sustained by GSH. In detail, 10 μ L of 200 mM ASC or 50 μ L of 100 mM GSH solution in ethanolamine-HCl buffer (pH 9.0) were added to the reaction tubes to yield the final concentrations of 2 mM ASC and 5 mM GSH. In these experiments the final NO_2^- concentration in the reaction medium was 10 mM. The employed GSH dose, roughly corresponding to GSH concentration in intact mammalian mitochondria [24,25], was the same as in a previous

work [26]. In these experiments, due to the possible formation of photosensitive *S*-nitrosothiols, both the preincubation of mitochondria and the subsequent ATPase assay were performed in parallel in the dark and in the light to allow comparison.

To evaluate the hydrogen peroxide (H_2O_2) effect on the nitrite-preincubated mitochondrial suspensions, 30% (w/w) H_2O_2 solution in H_2O was added to the reaction medium immediately before the ATPase assay to attain a final H_2O_2 concentration of $1 \mu\text{mol H}_2\text{O}_2/33 \mu\text{g}$ mitochondrial protein, which, even if higher than that currently reported in mitochondria [27], unaffected the ATPase activity. H_2O_2 scavengers, namely $50 \mu\text{M}$ dithiothreitol (DTT) or $100 \mu\text{M}$ α -Tocopherol (TOC), expressed as final concentrations in the reaction system, were added to the reaction mixture [27] to check any possible redox effect on the nitrite inhibition of the enzyme activity.

Different PTIO concentrations concomitantly added together with nitrite to mitochondria aimed at preventing $\cdot\text{NO}$ formation from nitrite [28].

All these treatments were made before starting the ATPase reaction.

2.4. Assay of the mitochondrial F-ATPase activity

Thawed mitochondrial fractions were immediately used for ATPase activity assays. Whenever a preincubation procedure was applied, immediately after the preincubation time, appropriate aliquots of the preincubated mitochondrial suspensions were sampled by a micropipette and directly added to the ATPase reaction media to yield the final concentration of $0.15 \text{ mg protein/mL}$.

The capability of ATP hydrolysis was assayed in a reaction medium (1 mL) containing 75 mM ethanolamine-HCl buffer pH 9.0, 0.15 mg mitochondrial protein plus 6.0 mM Na_2ATP and 2.0 mM MgCl_2 for the Mg-dependent F_1F_0 -ATPase assay (henceforth defined as Mg-ATPase(s) to account for the possible contribution of different ATPases), and 3.0 mM Na_2ATP and 2.0 mM CaCl_2 for the Ca-dependent F_1F_0 -ATPase assay (henceforth defined as Ca-ATPase(s), because several different ATPase may exist and function). These assay conditions were applied in all experiments, apart when otherwise stated in the Figure legends. After 5 min preincubation at $37 \text{ }^\circ\text{C}$, the reaction, carried out at the same temperature, was started by the addition of the substrate ATP and stopped after 5 min by the addition of 1 mL of ice-cold 15% (w/w) aqueous solution trichloroacetic acid. Once the reaction was stopped, vials were centrifuged for 15 min at 5000 rpm (ALC 4225 Centrifuge) [29]. In the supernatant, the concentration of inorganic phosphate (P_i) hydrolyzed by known amounts of mitochondrial protein, which is an indirect measure of ATPase activity, was spectrophotometrically evaluated according to Fiske and Subbarow [30].

The ATPase activity was routinely measured by subtracting, from the P_i hydrolyzed by known amounts of mitochondrial protein (which indirectly indicates the total ATPase activity), the P_i hydrolyzed in the presence of 3 $\mu\text{g}/\text{mL}$ oligomycin. To this aim, 1 μL from a mother solution of 3 mg/mL oligomycin in dimethylsulfoxide (DMSO) was directly added to the reaction mixture before starting the reaction. The total ATPase activity was calculated by detecting the P_i in control tubes run in parallel and containing 1 μL DMSO per mL reaction system. In each experimental set, control tubes were alternated to the condition to be tested. The employed dose of oligomycin, a specific inhibitor of F-ATPases which selectively blocks the F_0 subunit [24] ensured maximal enzyme activity inhibition and was currently used in ATPase assays [23,26]. In all experiments the ATPase activity was calculated as $\mu\text{moles } P_i \cdot \text{mg protein}^{-1} \cdot \text{h}^{-1}$.

2.5. Kinetic analyses

To calculate the kinetic parameters (V_{max} and K_m), data were fitted to the Michaelis-Menten equation using the program Grafit 7. The reaction rate was plotted as a function of the concentration of substrate.

The mechanism of the enzyme inhibition by nitrite was explored by the aid of the graphical methods of Dixon [31] and Cornish-Bowden [32], which complement one another [33]. In all kinetic analyses the enzyme specific activity was taken as the expression of the reaction rate (v). Briefly, to build Dixon plot the reciprocal of the reaction rate $1/v$ (y axis) was plotted as a function of the concentration of the inhibitor nitrite $[\text{NO}_2^-]$ (x axis). To build Cornish-Bowden plots, the ratio S/v , being S the millimolar concentration of ATP substrate, was plotted as a function of $[\text{NO}_2^-]$. In both cases, by plotting the enzyme activity data, distinct straight lines, each of which corresponded to a fixed concentration of substrate ATP at constant concentration of each cofactor (either Mg^{2+} or Ca^{2+}), were obtained by linear regression. The R^2 value were never lower than 0.9025, thus confirming the linearity of these plots [33]. At least three independent experiments were carried out to build each plot.

2.6. Quantitative evaluation of nitrotyrosine and dityrosine

The possible formation of nitrotyrosine and dityrosine in mitochondrial proteins in the presence of different nitrite concentrations, as post translational modification, was evaluated spectrophotometrically [34]. The selected nitrite concentrations in medium A were added to 300 μg mitochondrial suspensions and incubated for 30 min in ice before the analysis. In each set of

experiments the same volume of nitrite-free medium A was added in parallel to controls. Then, aliquots of preincubated mitochondrial suspensions were added to ethanolamine-HCl buffer, pH 10.0 to yield a final volume of 2.3 mL in the cuvette. After 1 min of acclimation at 37 °C under magnetic stirring, the absorbance was read at the spectrophotometer. On the same sample, by automatically changing the absorption wavelength, the nitrotyrosine content was evaluated by detecting the absorbance at 430 nm, while the dityrosine formation was calculated from the increase in absorbance at 330 nm. In each experiment set, according to the Lambert-Beer law, the absorbance values were converted to concentration values by exploiting the nanomolar extinction coefficients (ϵ) of nitrotyrosine ($\epsilon_{430\text{ nm}} = 4,400\text{ M}^{-1}\cdot\text{cm}^{-1}$), and dityrosine ($\epsilon_{330\text{ nm}} = 4,000\text{ M}^{-1}\cdot\text{cm}^{-1}$), respectively [34]. All data were expressed as nmol nitrotyrosine or dityrosine/mg mitochondrial protein.

2.7. Statistics

The data represent the mean \pm SD (shown as vertical bars in the figures) of the number of experiments reported in the figure captions and table legends. In each experimental set, the analyses were carried out on different pools of animals. The differences between data were evaluated by one way ANOVA followed by Students–Newman–Keuls’ test or two way ANOVA followed by Turkey’s test, when F values indicated significance ($P \leq 0.05$).

3. Results and Discussion

3.1 The mitochondrial Ca-ATPase activity/ies may refer to the F_1F_0 -complex

The reversible energy transducing mechanism of the mitochondrial F_1F_0 -complex couples the transmembrane Δp to ATP synthesis/hydrolysis [2]. The occurrence of a divalent cation, primarily Mg^{2+} , which is the natural cofactor, is essential for both ATP hydrolysis and ATP synthesis. However, Mg^{2+} can be replaced by several divalent metal cations including Ca^{2+} [35]. Consistently, in swine heart mitochondria, other than Mg^{2+} which stimulates the so-called Mg-ATPase activity/ies, also Ca^{2+} sustains the ATPase activity of the F_1F_0 complex, defined as Ca-ATPase(s), even if far less efficiently (Table 1). Accordingly, the maximal reaction rate (V_{\max}) of the Mg-ATPase(s) is about 3 times greater than that of the Ca-ATPase(s). Moreover, on considering the K_m values, the enzyme sensibility for Mg^{2+} is 5 times greater than that for Ca^{2+} (Table 1). As first step, to exclude the possibility that the detected Ca-ATPase activity/ies may result from a possible contamination of the mitochondrial preparations with other cellular components, the effect of various inhibitors which selectively act on other ATPases and that of oligomycin, a specific

inhibitor of the F_1F_0 -complex, were tested. Therefore, the ATPase activity was evaluated in the presence of either Mg^{2+} or Ca^{2+} plus one of the following inhibitors: 2,5-di-*tert*-butylhydroquinone (BHQ), vanadate and oligomycin. Each of these three inhibitors has specific targets. BHQ specifically inhibits the sarcoplasmic reticulum Ca^{2+} -ATPase at micromolar concentrations [36]. Vanadate, which structurally mimics inorganic phosphate (P_i), inhibits ion pumping by P-type ATPases such as the Na^+/K^+ -ATPase and the Ca^{2+} -ATPase; it targets the E_2 enzyme conformation within the membrane domain from the outer (extracellular) side and thus blocks cation release [37]. Finally, oligomycin is a known specific inhibitor of F_0 sector of F_1F_0 -ATPase [2,24,27]. The results obtained clearly show that both the Ca- and the Mg-ATPase activities are similarly unaffected by BHQ (Fig. 1A) and vanadate (Fig. 1B), whereas both ATPases are strongly inhibited by oligomycin (Fig. 1C). From a close insight, the IC_{50} values for oligomycin of 54.6 ± 2.8 ng/mL for the Ca-ATPase activity and of 68.5 ± 5.4 ng/mL for the Mg-ATPase activity are of the same magnitude order (Fig. 1C). Moreover, the linear portion of the dose response curves have overlapping slopes, namely 1.54 ± 0.11 for the Ca-ATPase(s) and 1.71 ± 0.20 for the Mg-ATPase(s). Finally, a similar background, corresponding to the residual oligomycin-resistant ATPase activity, is detected for the Ca-ATPase(s) and for the Mg-ATPase(s), namely 4.0 ± 0.7 $\mu\text{mol Pi mg protein}^{-1} \text{ hr}^{-1}$ and 5.9 ± 2.6 $\mu\text{mol Pi mg protein}^{-1} \text{ hr}^{-1}$, respectively. Thus, the whole of data strongly indicates that the ATPase activity sustained by Ca^{2+} has the same response to inhibitors as that activated by Mg^{2+} , being similarly inhibited by oligomycin and refractory to inhibitors of other ATPases as the F_1F_0 complex.

3.2. In search of a role of the mitochondrial Ca-ATPase activities

Other experiments aimed at enlightening the presumptive role of the ATPase activity elicited by Ca^{2+} in swine heart mitochondria. An increasing variety of membrane-bound divalent-cation activated ATPases has been described in mitochondria, and their function is still partially obscure [38]. On these bases we should not rule out the possibility that our experiments carried out in the presence of Ca^{2+} and in the absence of Mg^{2+} and *vice versa* elicited ATPase activities related to different protein structures, coexistent in mitochondrial membranes. Therefore a cautious use of the plural term of ATPases is somehow mandatory. However the pronounced oligomycin sensitivity of the ATPase activity under study indicates the F_1F_0 complex as the most likely candidate for the ATP hydrolysis sustained by Ca^{2+} pointed out in swine heart mitochondria. Previous studies on beef heart submitochondrial particles showed that Ca-ATPase activity had no proton pumping activity

and was oligomycin-insensitive [35], thus likely uncoupled to proton transport. Otherwise, in our experiments the swine heart mitochondrial Ca-dependent ATPase activity is clearly oligomycin-sensitive and most likely refers to the same mitochondrial F_1F_0 complex, activated by Ca^{2+} in replacement of Mg^{2+} . The ATP hydrolysis by F_1 is also probably coupled to proton translocation within F_0 as the Mg-ATPase activity [2], even if it should be taken into consideration that not necessarily all ATPase activities in mitochondria belong to the F_1F_0 -complex and respond to oligomycin. Otherwise, recent advances show that the proton current generated by Ca^{2+} -dependent F_1F_0 -ATPase is indistinguishable from that of MPTP [39]. In the mitochondrial matrix the co-occurrence of high Ca^{2+} concentrations, P_i and cyclophilin D (CyPD), a peptidyl-prolyl *cis-trans* isomerase endowed with the same CyP-like domain as CyP enzymes (CYPs), would favour MPT by reversibly opening MPTP. This proteinaceous pore, of unknown nature [10], is desensitized by cyclosporin A (CsA) [39,40], in turn chemical inhibitor of CyPD, the only mitochondrial CyP isoform in mammals and involved in MPT regulation. Interestingly, CyPD can electrostatically interact with the OSCP subunit of the F_1F_0 -ATPase in an overlapping region to the binding site of the inhibitor benzodiazepine 423, which enters mitochondria [41] and triggers the channel activity in F_1F_0 -ATPase dimers [9] which would constitute MPTP. Quite surprisingly, the natural inhibitor IF_1 , which promotes the F_1F_0 -ATPase dimerization, decreases MPTP opening and reduces I/R injury [42]. The whole pattern is quite confused and contradictory, so it seemed worthwhile testing CsA effects on the ATPase activities in freeze-thawed mitochondria in which the transmembrane electrochemical gradient is abolished and no osmotic swelling occurs. This protocol aimed at evaluating the direct effect of CsA on the enzyme activities. Interestingly, when activated by Mg^{2+} the ATPase activity is not affected by CsA even beyond pharmacologically relevant concentrations, whereas when activated by Ca^{2+} the enzyme activity is 30% reduced (Fig. 2). Moreover, the enzyme inhibition by CsA is apparently enhanced by an increase in Ca^{2+} concentration (Fig. 2). Thus, the ATPase activity stimulated by Ca^{2+} , even if sustained by the same F_1F_0 complex as the classical Mg-dependent ATPase activity, may possess peculiar cofactor-dependent features, may be related to its putative involvement with MPTP [40].

3.3. Nitrite especially inhibits the ATPase activity when the activating cation is Ca^{2+}

The ATPase responses to nitrite add further distinguishing features. Nitrite *per se* is a physiologically inert end product of $\cdot NO$ metabolism which can act as endocrine $\cdot NO$ reservoir in blood and tissues [15,17]. During hypoxia nitrite is involved in an intricate scavenger system [12, 14-17] and the subcellular nitrite targets are not completely elucidated yet. Nitrite reduction to $\cdot NO$

or even to more critical products in biomolecules occurs in mitochondria although it seems unlikely that nitrite can cross the membrane by free diffusion [43], since only 10% of nitrite added to isolated mitochondria is internalized [44]. Experiments carried out to evaluate the Mg-ATPase and Ca-ATPase activities under different assay conditions can help to discriminate between different nitrite effects, tightly dependent on the cation which acts as cofactor (Fig. 3). Even if the biological effects of nitrite are usually reported at micromolar concentrations [14], we tested a wide range of nitrite concentrations, from 100 μM to 10 mM nitrite, which are clearly higher than that found in mammalian tissues [45], to allow nitrite incorporation in the mitochondrial membrane and shed light on the different response of the two differently activated ATPase activities. Micromolar concentrations of nitrite, which do not affect the Mg-ATPase(s), cause a significant decrease in the Ca-ATPase activity/ies (Figure 3). In practice the activity of the Mg-ATPase(s) is unaltered by up to 2 mM nitrite and only 35% inhibited by 10 mM nitrite, whereas the Ca-ATPase activity is much more responsive to nitrite and halved by 5-10 mM nitrite (Fig. 3). Since nitrate (NO_3^-) is ineffective at low concentrations and only inhibits the Ca-ATPase(s) at >5 mM (Fig. S1), the enzyme inhibition by nitrite seems unrelated to nitrate. The inhibition constant (K'_i) of the Mg-ATPase and Ca-ATPase activities can be taken as somehow indicative of the bond strength between the inhibitor and the enzyme complex. As shown by Dixon and Cornish-Bowden plots, in both cases nitrite acts as uncompetitive inhibitor, namely it only binds to the enzyme-ATP complex (ES) (Fig. 4). Interestingly, the affinity for nitrite of the Ca-ATPase(s) is about 20 times greater than that of the Mg-ATPase(s), as shown by the K'_i values of 0.9 mM for Ca-ATPase(s) (Fig. 4B) and of 16.7 mM for Mg-ATPase(s) (Fig. 4D).

3.4. In search of the molecular inhibition mechanism of nitrite

Once assessed that the Ca-ATPase activity is most likely a peculiar operating mode of the F_1F_0 -complex, especially sensitive to nitrite, the inhibitory mechanism of nitrite was further investigated at the molecular level aiming at defining the chemical mode of inhibition of the enzyme activity. Since the Ca-ATPase inhibition by 1 mM nitrite is not affected by the preincubation pH in the physiological range 6.6–7.8 (data not shown), nitrite protonation (which may occur at mildly acidic incubation pH) is not involved in the ATPase inhibition.

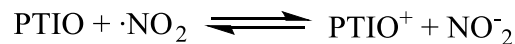
Chemical and/or enzymatic formation of nitrite redox products may lead to *S*-nitrosation (*S*-nitrosylation) of critical thiol residues on the F_1F_0 complex, as proven for mitochondrial respiratory chain complexes [46, 47]. To check this possibility, experiments were carried out in the presence of

ascorbate (ASC) (Fig. 5), a reagent known to reduce *S*-nitrosothiols at 2 mM concentration [48]. Moreover, since the formation of *S*-nitrosothiols could be facilitated by transnitrosation reactions [48], in which the nitrosonium ion (NO^+) is transferred from one thiol to another by means of a low molecular weight thiol (*e.g.* GSH) which acts as transient intermediate, GSH addition aimed at favouring this mechanism. The results from different sets of experiments, collectively shown in Fig. 5, clearly indicate that ASC individually tested or as binary mixture with GSH increases ATP hydrolysis, whereas GSH *per se* does not modify the Ca-ATPase activities (control). Above all, the compounds tested are absolutely ineffective on the Ca-ATPase inhibition by nitrite. The overlapping results obtained in experiments carried out the light and in the dark (data not shown) are fully consistent with the lack of photosensitive *S*-nitrosothiols. The whole of data rules out the possibility that the nitrite inhibition of the Ca-ATPase activity/ies involves *S*-transitrosation of critical enzyme thiols.

Nitration and amino acid radicals stem from post-translational modifications of proteins promoted by several reagents including nitrite in the presence of H_2O_2 /peroxidases [44,49]. To check this possibility, the effect of 10 mM nitrite on the ATPase activities raised either by Ca^{2+} or by Mg^{2+} was evaluated in the presence and in the absence of H_2O_2 (Fig. 6). While H_2O_2 has no effect on the ATPase activities, irrespective of the activating cation, it clearly enhances the ATPase inhibition by nitrite in both cases. The promotion of nitrosative stress in mitochondria, namely the generation of nitrogen radical species such as nitrogen dioxide ($\cdot\text{NO}_2$), from peroxidase-catalyzed nitrite oxidation by H_2O_2 [49] could be involved. In order to verify the protein redox state, the thiol reagent DTT and the antioxidant α -tocopherol (TOC) were tested. DTT can reduce accessible sulfides and thus reestablish thiol state in proteins if no irreversible *S*-modifications (*e.g.* sulfinic or sulfonic acids) occur, while TOC can efficiently neutralize the H_2O_2 -borne radicals. Since both reagents do not affect nitrite inhibition of the Ca-ATPase(s) (Fig. 6), irrespective of the H_2O_2 presence, nitrite is likely to promote redox-insensitive post-translational modifications on the ATPase(s).

Another inhibition mechanism was explored, namely the possible reduction of nitrite to $\cdot\text{NO}$ in mitochondria. In this case, nitrite would act as indirect responsible for the ATPase inhibition while $\cdot\text{NO}$ would act directly. To check this possibility, $\cdot\text{NO}$ formation must be prevented by PTIO, a reagent which as other nitronyl nitroxides is currently exploited to eliminate $\cdot\text{NO}$. Not only PTIO is a selective spin $\cdot\text{NO}$ trap, but also it can produce nitrite [28]. Experiments carried out by incubating mitochondria with nitrite in the presence of increasing PTIO concentrations (Figure 7) clearly show that the Ca-ATPase inhibition by nitrite is unaffected by PTO, thus ruling out any involvement of $\cdot\text{NO}$ radical. Therefore, alternative mechanisms were explored. PTIO reacting with $\cdot\text{NO}$ can

produce the corresponding imino-nitroxide and the radical $\cdot\text{NO}_2$, a potential candidate as post-translational modifier of mitochondrial proteins. In this case, assumed that the $\cdot\text{NO}_2$ radical stems from $\cdot\text{NO}$, in turn obtained by nitrite reduction, PTIO would enhance the Ca-ATPase inhibition, but no enhancement of the enzyme inhibition was shown (Fig. 7). Consistently, it seems reasonable to speculate that the PTIO reacts with $\cdot\text{NO}_2$ and produces oxoammonium cation (PTIO^+) and nitrite, according to the reversible reaction:



in which the forward reaction decreases the radical concentration, whereas the reverse reaction produces the radical $\cdot\text{NO}_2$. To verify the possible involvement of this radical species, the effects of 10 mM and 1 mM nitrite were tested. Accordingly, in the presence of 10 mM nitrite (high nitrite concentration), the equilibrium is presumptively shifted to the left, maintaining the nitrosative species $\cdot\text{NO}_2$ in the reaction system. Conversely, low (1 mM) nitrite concentrations will shift the reaction to the right and minimize $\cdot\text{NO}_2$ concentration. However, since even low (1 mM) nitrite concentrations do not modify the inhibition extent in the presence of PTIO, any PTIO^+ reaction with nitrite is not likely.

Modification of tyrosine residues by nitrite can lead to the formation of nitrotyrosine and/or dityrosine [50]. To discriminate between these two possibilities, we evaluated both nitrotyrosine and dityrosine contents in mitochondria incubated with increasing nitrite concentrations. The results shown in Fig. 8 indicate that nitrite only promotes a significant formation of dityrosine above 5 mM while the level of nitrotyrosines is in practice not detectable. The failed detection of nitrotyrosine, which could correspond to a lack of this nitrite-driven modification, is consistent with previous reports [51] on the nitration of specific tyrosine residues. Accordingly, the nitration of two distinct Tyr residues (Tyr³⁴⁵ and Tyr³⁶⁸) on F₁F₀-ATPase β -subunit was reported to inactivate the enzyme, because the nitro group caused steric hindrance and changed the phenolic pK_a. In detail, Tyr³⁶⁸ is four times more prone to nitration than Tyr³⁴⁵, due to its lower pK_a [50]. Upon nitration, Tyr³⁴⁵ positioned near the Walker A motif, the nucleotide binding site, alters the hydrophobic pocket containing the adenosine of ATP sandwiched between the two aromatic rings of Tyr³⁴⁵ and Phe⁴²⁴ [52]. The failed inhibition of the ATPase activity by low nitrite concentrations (Fig. 3B) is consistent with the hypothesized absence of nitrotyrosine, which would inhibit the F₁F₀-ATPase activity [51]. The dityrosine formation seems to be especially deleterious for the ATPase activity sustained by Ca²⁺.

3.5. The putative mechanism of ATPase inhibition by nitrite

To sum up and visualize the mechanisms involved in nitrite inhibition, Fig. 9 illustrates the main findings: nitrite more effectively inhibits the Ca-ATPase(s) (Fig. 9A) than the Mg-ATPase(s) (Fig. 9C); the ATPase inhibition by nitrite is strengthened by H₂O₂ both when the enzyme activity is Ca²⁺-dependent (Fig. 9B) and also, to a lower extent, when the enzyme activity is Mg²⁺-dependent (Fig. 9D). Assumed that ATP hydrolysis is coupled to proton pumping, most likely the effects on the ATPase activity parallel those on uphill proton fluxes across the IMM from the matrix to the intermembrane space. On the bases of present knowledge, a putative chemical mechanism by which nitrite leads to the formation of dityrosine can be depicted. Nitrite would possess both anti- and pro-oxidant activities by interfering in peroxidase or heme-dependent redox reactions. Due to oxidative stress, a mitochondrial peroxidase can loss two-electrons [25]; in turn nitrite can transfer one electron to the enzyme to form the radical ·NO₂ [52]. The latter, a potent oxidizing and nitrating agent, can promote tyrosine nitration in proteins accompanied by the formation of other radical species [53]. The addition of a second radical ·NO₂ to the tyrosyl radical could lead to nitrotyrosine formation. However, most likely, during ATP hydrolysis two adjacent tyrosyl radicals bind together to form dityrosine (Fig. 9E). Furthermore, the uncompetitive inhibition mechanism (Figure 4) implies that nitrite binds to the enzyme-ATP complex (ES). Therefore, the enzyme inhibition may result from a two-step post-translational modification, namely the nitrite-driven generation of tyrosyl radicals and the concomitant formation of the ES complex and of dityrosine. Accordingly, the conformational change of the catalytic sites by binding change mechanism [1,54] occurring during the ATP hydrolysis by the F₁F₀-complex, could enable the tyrosyl radicals, produced during the preincubation of mitochondria with nitrite, to get closer to make them covalently bind together by connecting the two aromatic radicals (Fig. 9E).

4. Conclusion

Assumed that the depicted molecular mechanisms are similarly operative *in vitro* and *in vivo*, it is really intriguing to imagine how the present findings could partially explain the beneficial effects of nitrite, which modulates the mitochondrial functions at various levels [14,15], to counteract cardiovascular diseases. The hypothesized mechanisms by which nitrite would act differently on the mitochondrial F₁F₀-complex, according to the cation which acts as a cofactor, may represent a protective enzymatic strategy to limit cellular death and cytotoxicity at reperfusion in the mammalian heart, liver, and brain. Accordingly, assumed that both Ca²⁺ and Mg²⁺ elicit ATPase activities referable to the same F₁F₀-complex, when the enzyme complex switches to the Ca²⁺-

activated mode, it may undergo nitrite effects and decrease catalysis. Under pathophysiological conditions in which calcium concentration increases in the mitochondrial matrix, the IMM is depolarized [39] and the F_1F_0 -ATPase works “in reverse”, namely in the direction of ATP hydrolysis [3,54]. Under such conditions, elevated nitrite concentrations *in vivo* may selectively inhibit the ATPase activity sustained by Ca^{2+} without affecting that activated by Mg^{2+} , thus counteracting the negative events linked to the calcium dependent functioning mode of the F_1F_0 complex.

Acknowledgements

This work was financed by a RFO grant from the University of Bologna, Italy.

Danilo Matteuzzi (Department of Veterinary Medical Sciences, University of Bologna) is gratefully acknowledged for kindly conferring pig hearts from a local abattoir to our lab.

References

- [1] P.D. Boyer, A perspective of the binding change mechanism for ATP synthesis, *FASEB J.* 3 (1989) 2164-78.
- [2] J.E. Walker, The ATP synthase: the understood, the uncertain and the unknown, *Biochem. Soc. Trans.* 41 (2013) 1-16.
- [3] G.I. Grover, G.J.J. Malm, Pharmacological profile of the selective mitochondrial F_1F_0 ATP hydrolase inhibitor BMS-1999264 in myocardial ischemia, *Cardiovasc. Ther.* 26 (2009) 287-96.
- [4] W. Junge, H. Sielaff, S. Engelbrecht, Torque generation and elastic power transmission in the rotary $F(O)F(1)$ -ATPase, *Nature* 459 (2009) 364-70.
- [5] S. Nesci, F. Trombetti, V. Ventrella, A. Pagliarani, Opposite rotation directions in the synthesis and hydrolysis of ATP by the ATP synthase: hints from *a* subunit asymmetry, *J. Membr. Biol.* 248 (2015) 163-9.
- [6] M. Bonora, M.R. Wieckowski, C. Chinopoulos, O. Kepp, G. Kroemer, L. Galluzzi, P. Pinton, Molecular mechanisms of cell death: central implication of ATP synthase in mitochondrial permeability transition, *Oncogene* 34 (2015) 1608.
- [7] S. Nesci, V. Ventrella, F. Trombetti, M. Pirini, A. Pagliarani, Thiol oxidation of mitochondrial F_0 -c subunits: a way to switch off antimicrobial drug targets of the mitochondrial ATP synthase, *Med. Hypotheses* 83 (2014) 160-165.

- [8] M. Bonora, A. Bononi, E. De Marchi, C. Giorgi, M. Lebiezinska, S. Marchi, S. Patergnani, A. Rimessi, J.M. Suski, A. Wojtala, M.R. Wieckowski, L. Galluzzi, P. Pinton, Role of the *c* subunit of the F₀ ATP synthase in mitochondrial permeability transition, *Cell Cycle* 12 (2013) 674-83.
- [9] V. Giorgio, S. von Stockum, M. Antoniel, A. Fabbro, F. Fogolari, M. Forte, G.D. Glick, V. Petronilli, M. Zoratti, I. Szabó, G. Lippe, P. Bernardi, Dimers of mitochondrial ATP synthase form the permeability transition pore, *Proc. Natl. Acad. Sci. USA* 110 (2013) 5887-92.
- [10] J. Karch, J.D. Molkenin, Identifying the components of the elusive mitochondrial permeability transition pore, *Proc. Natl. Acad. Sci. USA* 111 (2014) 10396-7.
- [11] K.N. Alavian, G. Beutner, E. Lazrove, S. Sacchetti, H.A. Park, P. Licznanski, H. Li, P. Nabili, K. Hockensmith, M. Graham, G.A.Jr. Porter, E.A. Jonas, An uncoupling channel within the *c*-subunit ring of the F₁F₀ ATP synthase is the mitochondrial permeability transition pore, *Proc. Natl. Acad. Sci. USA* 111 (2014) 10580-5.
- [12] D. Murillo, C. Kanga, L. Mo, S. Shiva, Nitrite as a mediator of ischemic preconditioning and cytoprotection, *Nitric Oxide* 25 (2011) 70-80.
- [13] H. Parlakpınar, M.H. Orum, M. Sagir, Pathophysiology of myocardial ischemia-reperfusion injury. A review, *Med-Science* 2 (2013) 935-54.
- [14] S. Shiva, M.T. Gladwin, Nitrite mediates cytoprotection after ischemia/reperfusion by modulating mitochondrial function, *Basic Res. Cardiol.* 104 (2009) 113-9.
- [15] S. Shiva, Nitrite: a physiological store of nitric oxide and modulator of mitochondrial function, *Red. Biol.* 1 (2013) 40-44.
- [16] S. Lidder, A.J. Webb, Vascular effects of dietary nitrate (as found in green leafy vegetables and beetroot) via the nitrate-nitrite-nitric oxide pathway, *Br. J. Clin. Pharmacol.* 75 (2013) 677-96.
- [17] E. Curtis, L.L. Hsu, A.C. Noguchi, L. Geary, S. Shiva, Oxygen regulates tissue nitrite metabolism, *Antiox. Redox Sign.* 17 (2012) 951-61.
- [18] S.A. Omar, A.J. Webb, Nitrite reduction and cardiovascular protection, *J. Mol. Cell Cardiol.* 73 (2014) 57-69.
- [19] C.B. Parrillo, S. Bir, V. Rajaram, C.G. Kevil, Inorganic nitrite and chronic tissue ischaemia: a novel therapeutic modality for peripheral vascular diseases, *Cardiovasc Res.* 89 (2011), 533-541.
- [20] M. Habermeyer, A. Roth, S. Guth, P. Diel, K.H. Engel, B. Epe, P. Fürst, V. Heinz, H.U. Humpf, H.G. Joost, D. Knorr, T. de Kok, S. Kulling, A. Lampen, D. Marko, G. Rechkemmer, I. Rietjens, R.H. Stadler, S. Vieths, R. Vogel, P. Steinberg, G. Eisenbrand, Nitrate and nitrite in the diet: how to assess their benefit and risk for human health, *Mol. Nutr. Food Res.* 59 (2015) 106-28.

- [21] F. Pellotti, G. Lenaz, Isolation and subfractionation of mitochondria from animal cells and tissue culture lines, *Methods Cell Biol.* 80 (2007) 3-44.
- [22] M.M. Bradford, A rapid and sensitive method for the quantitation of microgram quantities of protein utilizing the principle of protein-dye binding, *Anal. Biochem.* 72 (1976) 248-254.
- [23] S. Nesci, V. Ventrella, F. Trombetti, M. Pirini, A. Pagliarani, Thiol oxidation is crucial in the desensitization of the mitochondrial F_1F_0 -ATPase to oligomycin and other macrolide antibiotics, *Biochim. Biophys. Acta* 1840 (2014) 1882-91.
- [24] D.G. Nicholls, S.J. Ferguson, *Bioenergetics 4*, fourth ed., Academic Press, Amsterdam, 2013.
- [25] V. Ribas, C. Garcia-Raiz, J.C. Fernandez-Checa, Glutathione and mitochondria, *Front. Pharmacol.* 5 (2014) 151.
- [26] A. Boveris, E. Cadenas, Mitochondrial production of hydrogen peroxide regulation by nitric oxide and the role of ubisemiquinone, *IUBMB Life* 50 (2000) 245-250.
- [27] S. Nesci, V. Ventrella, F. Trombetti, M. Pirini, A. Pagliarani, The mitochondrial F_1F_0 -ATPase desensitization to oligomycin by tributyltin is due to thiol oxidation, *Biochimie* 97 (2014) 128-37.
- [28] S. Goldstein, A. Russo, A. Samuni, Reactions of PTIO and carboxy-PTIO with NO , $\cdot NO_2$, and O_2^- , *J. Biol. Chem.* 278 (2003) 50949-55.
- [29] S. Nesci, V. Ventrella, F. Trombetti, M. Pirini, A. Pagliarani, Mussel and mammalian ATP synthase share the same bioenergetic cost of ATP, *J. Bioenerg. Biomembr.* 45 (2013) 289-300.
- [30] C.G. Fiske, Y. Subbarow, The colorimetric determination of phosphorus, *J. Biol. Chem.* 66 (1925) 375-400.
- [31] M. Dixon, E.C. Webb, *Enzymes*, third ed., Academic Press, New York, 1979.
- [32] A. Cornish-Bowden, A simple graphical method for determining the inhibition constants of mixed, uncompetitive and non-competitive inhibitors, *Biochem. J.* 137 (1974) 143-144.
- [33] S. Nesci, V. Ventrella, F. Trombetti, M. Pirini, A.R. Borgatti, A. Pagliarani, Tributyltin (TBT) and dibutyltin (DBT) differently inhibit the mitochondrial Mg-ATPase activity in mussel digestive gland, *Toxicol. In Vitro* 25 (2011) 117-24.
- [34] H. Ischiropoulos, A.B. al-Mehdi, Peroxynitrite-mediated oxidative protein modifications, *FEBS Lett.* 364 (1995) 279-82.
- [35] S. Papageorgiou, A.B. Melandri, G. Solaini, Relevance of divalent cations to ATP-driven proton pumping in beef heart mitochondrial F_0F_1 -ATPase, *J. Bioenerg. Biomembr.* 30 (1998) 533-41.

- [36] A.A. Kabbara, D.G. Stephenson, Effects of 2,5-di-tert-butylhydroquinone on rat cardiac muscle contractility, *Am. J. Physiol.* 272 (1997) H1001-10.
- [37] M. Aureliano, G. Fraqueza, C.A. Ohlin, Ion pumps as biological targets for decavanadate, *Dalton Trans* 42 (2013) 11770-7.
- [38] Li S., D. Rouseau. ATAD3, a vital membrane bound mitochondrial ATPase involved in tumor progression, *J. Bioenerg.Biomembr.* 22 (2012) 189-197.
- [39] M. Antoniel, V. Giorgio, F. Fogolari, G.D. Glick, P. Bernardi, G. Lippe, The oligomycin-sensitivity conferring protein of mitochondrial ATP synthase: emerging new roles in mitochondrial pathophysiology, *Int. J. Mol. Sci.* 15 (2014) 7513-36.
- [40] P. Bernardi, The mitochondrial permeability transition pore: a mystery solved? *Front. Physiol.* 4 (2013) 95.
- [41] A.C. Stelzer, R.W. Frazee, C. Van Huis, J. Cleary, A.W. Jr. Opipari, G.D. Glick, H.M. Al-Hashimi, NMR studies of an immunomodulatory benzodiazepine binding to its molecular target on the mitochondrial F(1)F(0)-ATPase, *Biopolymers* 93 (2010) 85-92.
- [42] D. Faccenda, C.H. Tan, A. Seraphim, M.R. Duchon, M. Campanella, IF1 limits the apoptotic-signalling cascade by preventing mitochondrial remodeling, *Cell. Death. Differ.* 20 (2013) 686-97.
- [43] S. Shiva, Mitochondria as metabolizers and targets of nitrite, *Nitric Oxide* 22 (2010) 64-74.
- [44] P.R. Castello, D.K. Woo, K. Ball, J. Wojcik, L. Liu, R.O. Poyton, Oxygen-regulated isoforms of cytochrome c oxidase have differential effects on its nitric oxide production and on hypoxic signaling, *Proc. Natl. Acad. Sci. USA* 105 (2008) 8203-08.
- [45] P. Keigenboard, A. Dejan, T. Lauer, T. Rassal, A. Schindler, O. Picker, T. Scheeren, A. Gödecke, J. Schrader, R. Schultz, G. Heusch, G.A. Schaub, N.S. Bryan, M. Feelish, M. Kelm, Plasma nitrite reflects constitutive nitric oxide synthase activity in mammals, *Free Rad. Biol. Med.* 36 (2003) 790-796.
- [46] S. Shiva, M.N. Sack, G.J. Greer, M. Duranski, L.A. Ringwood, L. Burwell, X. Wang, P. MacArthur, A. Shoja, N. Raghavachari, J.W. Calverst, P.S. Brookes, D.J. Lefer, M.T. Gladwin, Nitrite augments tolerance to ischemia/ reperfusion injury via the modulation of mitochondrial electron transfer, *J. Exp. Med.* 3 (2007) 2089-2102.
- [47] C.A. Piantadosi, Regulation of mitochondrial processes by protein S-nitrosylation, *Biochim. Biophys. Acta* 1820 (2012) 712-721.
- [48] B. Derakhshan, P.C. Wille, S.S. Gross, Unbiased identification of cysteine S-nitrosylation sites on proteins, *Nat. Protoc.* 2 (2007) 1685-91.

- [49] M. Feelisch, B.O. Fernandez, N.S. Bryan, M.F. Garcia-Saura, S. Bauer, D.R. Whitlock, P.C. Ford, D.R. Janero, J. Rodriguez, H. Ashrafian, Tissue processing of nitrite in hypoxia: an intricate interplay of nitric oxide-generating and -scavenging systems, *J. Biol. Chem.* 283 (2008) 33927–34.
- [50] S. Herold, Nitrotyrosine, dityrosine, and nitrotryptophan formation from metmyoglobin, hydrogen peroxide, and nitrite, *Free Radic. Biol. Med.* 36 (2004) 565-79.
- [51] Y. Fujisawa, K. Kato, C. Giulivi, Nitration of tyrosine residues 368 and 345 in the beta-subunit elicits F_0F_1 -ATPase activity loss, *Biochem. J.* 423 (2009) 219-31.
- [52] D.M. Rees, M.G. Montgomery, A.G. Leslie, J.E. Walker, Structural evidence of a new catalytic intermediate in the pathway of ATP hydrolysis by F_1 -ATPase from bovine heart mitochondria, *Proc. Natl. Acad. Sci. USA* 109 (2012) 11139-43.
- [53] L. Castro, V. Demicheli, V. Tórtora, R. Radi, Mitochondrial protein tyrosine nitration, *Free Radic. Res.* 45 (2011) 37-52.
- [54] P.D. Boyer, The ATP synthase: a splendid molecular machine, *Annu. Rev. Biochem.* 66 (1997) 717-49.

Figure captions

Figure 1. Mitochondrial F_1 -ATPase response to the inhibitors BHQ (A), vanadate (B) and oligomycin (C). The ATPase activities were assayed in the presence of 2 mM Mg^{2+} (\circ) or 2 mM Ca^{2+} (\bullet). The reaction was started by 6 mM Na_2ATP for the Mg -ATPase(s) and by 3 mM Na_2ATP for the Ca -ATPase(s) (A and B) and by 3 mM Na_2ATP in both cases (C). Each point represents the mean value \pm SD (vertical bars) of three experiments carried out on distinct pools.

Figure 2. F_1F_0 -ATPase sensitivity to CsA. The ATPase activities were assayed in the presence of 2 mM Mg^{2+} in a Ca^{2+} -free medium for the Mg -ATPase(s) (\bullet) and in a Mg^{2+} -free medium in the presence of 0.25 mM Ca^{2+} (\circ), or 2.0 mM Ca^{2+} for the Ca -ATPase(s) (\square) at increasing CsA concentrations. Each point represents the mean value \pm SD (vertical bars) of three experiments carried out on distinct pools.

Figure 3. Effect of nitrite on the mitochondrial ATPase activities activated by 2 mM Ca^{2+} , defined as Ca -ATPase(s) (\circ) or by 2 mM Mg^{2+} , defined as Mg -ATPase(s) (\bullet). In all cases the reaction was

started by 3 mM Na₂ATP. All points represent the mean \pm SD (vertical bars) of three distinct experiments.

Figure 4. Nitrite inhibition mechanism on the mitochondrial F₁F₀-ATPase activities. (A) Dixon plots of the Ca-ATPase(s) evaluated at 3.0 (●) and 1.5 mM ATP (○); (B) Cornish-Bowden plots of the Ca-ATPase(s) at 3 mM (■) and 1.5 mM ATP (□). (C) Dixon plots of the Mg-ATPase(s) evaluated at 3 mM ATP (○) and 6 mM ATP (●); (D) Cornish-Bowden plots of the Mg-ATPase(s) at 3 mM ATP (□) and 6 mM ATP (■). Details of these graphical methods are given in the Section “Kinetic analyses”. Each point represents the mean value \pm SD (vertical bars) of three experiments carried out on distinct pools

Figure 5. Evaluation of the possible *S*-nitrosylation involvement in the inhibition of the mitochondrial Ca-ATPase(s) by nitrite (NO₂⁻). The Ca-ATPase activity was assayed in the presence of 2 mM ASC, 5 mM GSH and 10 mM NO₂⁻, or of their combinations as indicated near each bar. The ATPase activities are expressed as % of the enzyme activity detected in the absence of ASC, GSH and NO₂⁻ (control). All points represent the mean \pm SD (vertical bars) of three distinct experiments. Different letters indicate significantly different values ($P \leq 0.05$).

Figure 6. Combined H₂O₂ and nitrite (NO₂⁻) effects on the Ca-ATPase (A) and on the Mg-ATPase activities (B) in the presence and in the absence of H₂O₂ scavengers. H₂O₂, NO₂⁻ and H₂O₂ + NO₂⁻ mixtures were tested, in the absence of DTT and TOC (green bar), and in the presence of 50 μ M DTT (red bar) or 100 μ M TOC (yellow bar) as detailed in the Methods Section. Both in A and in B the ATPase activities after preincubation in the absence of H₂O₂ and nitrite are taken as control. In each panel different letters indicate significant differences ($P \leq 0.05$) among the preincubation treatments indicated on the y axis (capital letters) or within each preincubation treatment (lower case letters). Data are the mean \pm SD (vertical bars) of three different experiments carried out on distinct pools.

Figure 7. Effect of PTIO on the Ca-ATPase activities. The ATPase activities were evaluated in the absence (control) (○) and in the presence of 1 mM (◇) or 10 mM nitrite (□) at increasing PTIO concentrations (logarithmic scale). Each point represents the mean value \pm SD (vertical bars) of three distinct experiments.

Figure 8. Evaluation of tyrosine post-translational modifications triggered by increasing nitrite concentrations in mitochondria. Dityrosine (●) nitrotyrosine (○). Each point represents the mean value \pm SD (vertical bars) of three experiments carried out on distinct pools. * indicates significant differences from the control (nitrite-free) ($P \leq 0.05$).

Figure 9. Models of the presumptive nitrite effects on the mitochondrial F_1F_0 -complex. Left panel: nitrite effects on the Ca-ATPase activity/ies in the absence (A) and in the presence of H_2O_2 (B) and on the Mg-ATPase activities in the absence (C) and in the presence of H_2O_2 (D). The enzyme inhibition is indicated by \downarrow . The line width is roughly indicative of the extent of the effect. The dashed curves indicate poor ATPase activities and H^+ fluxes. Right panel (E): the likely reaction sequence involved in dityrosine formation. From the top to the bottom: in the presence of H_2O_2 the mitochondrial peroxidase loses two-electrons and accepts one electron from nitrite forming the nitrogen dioxide radical ($\cdot NO_2$); in turn $\cdot NO_2$ promotes the formation of radical tyrosine species in the F_1F_0 -ATPase; the tyrosyl radical is stabilized by resonance (the different limit structures are within square brackets); two adjacent tyrosyl radicals within the catalytic domain of F_1F_0 -ATPase bind together to form dityrosine (Fig. 8E).

Figure S1 (Supplementary material). Effect of nitrate on the mitochondrial Ca-ATPase activity/ties. Data are the mean \pm SD (vertical bars) of three distinct experiments.

Table 1. Kinetic parameters of the divalent ion-dependent F₁F₀-ATPase.

F ₁ F ₀ -ATPase	Mg ²⁺ -dependent	Ca ²⁺ -dependent
V _{max} (μmol P _i ·mg protein ⁻¹ ·h ⁻¹)	171.8±12.6	51.0±2.3
K _m (mM)	0.12±0.04	0.62±0.09

Data are the mean ±SD of 3 determinations carried out on different tissue pools.

Figure 1

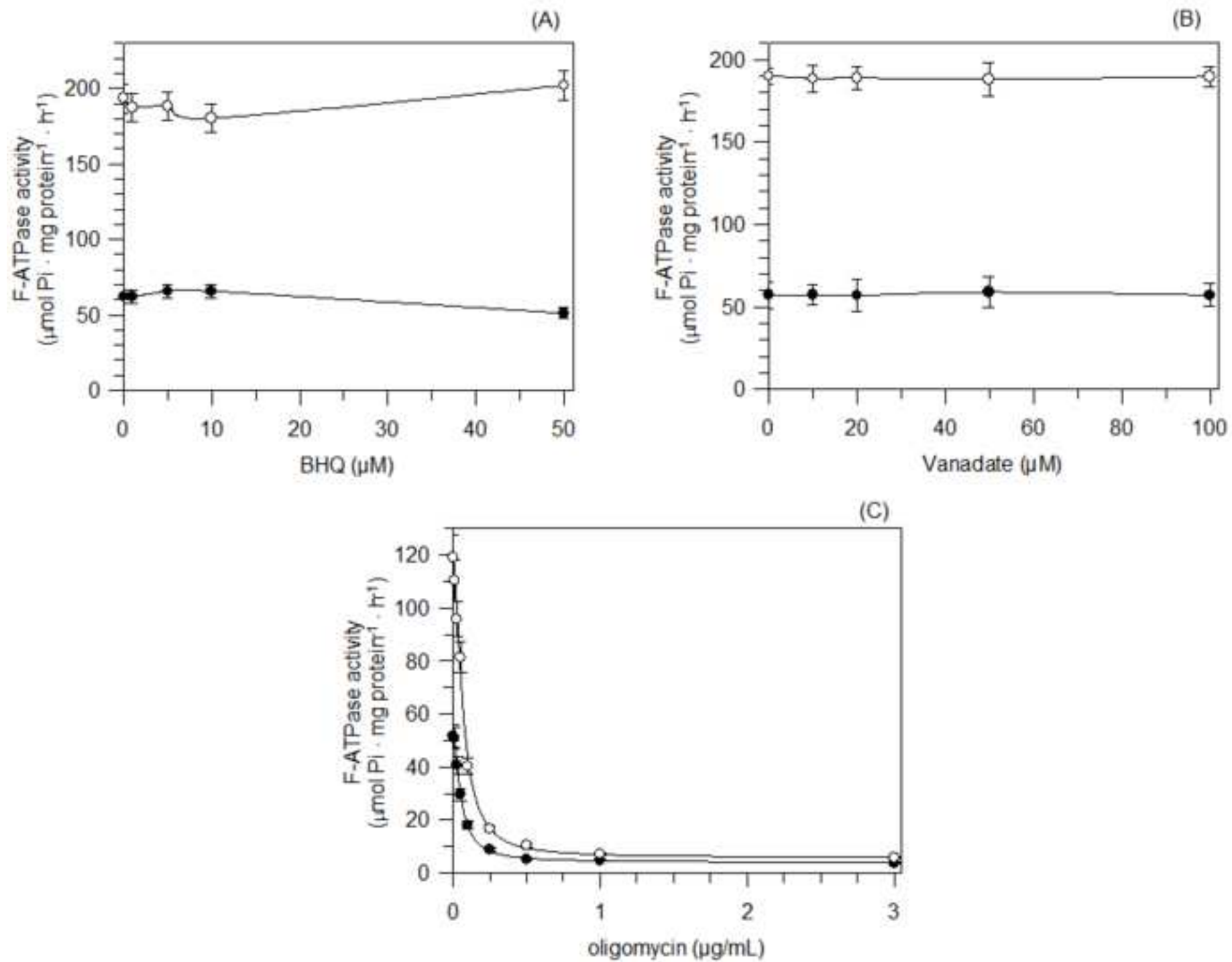


Figure 2

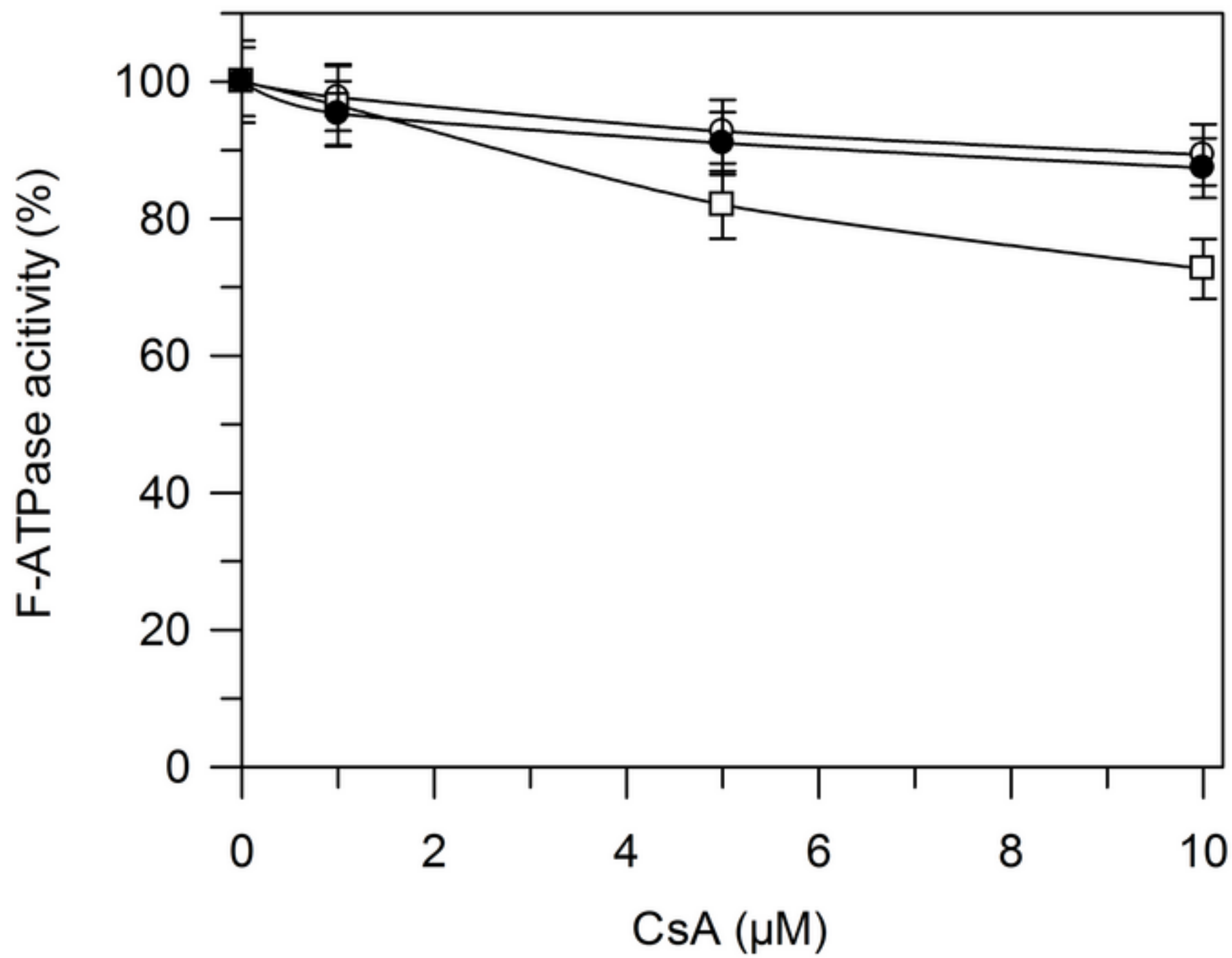


Figure 3

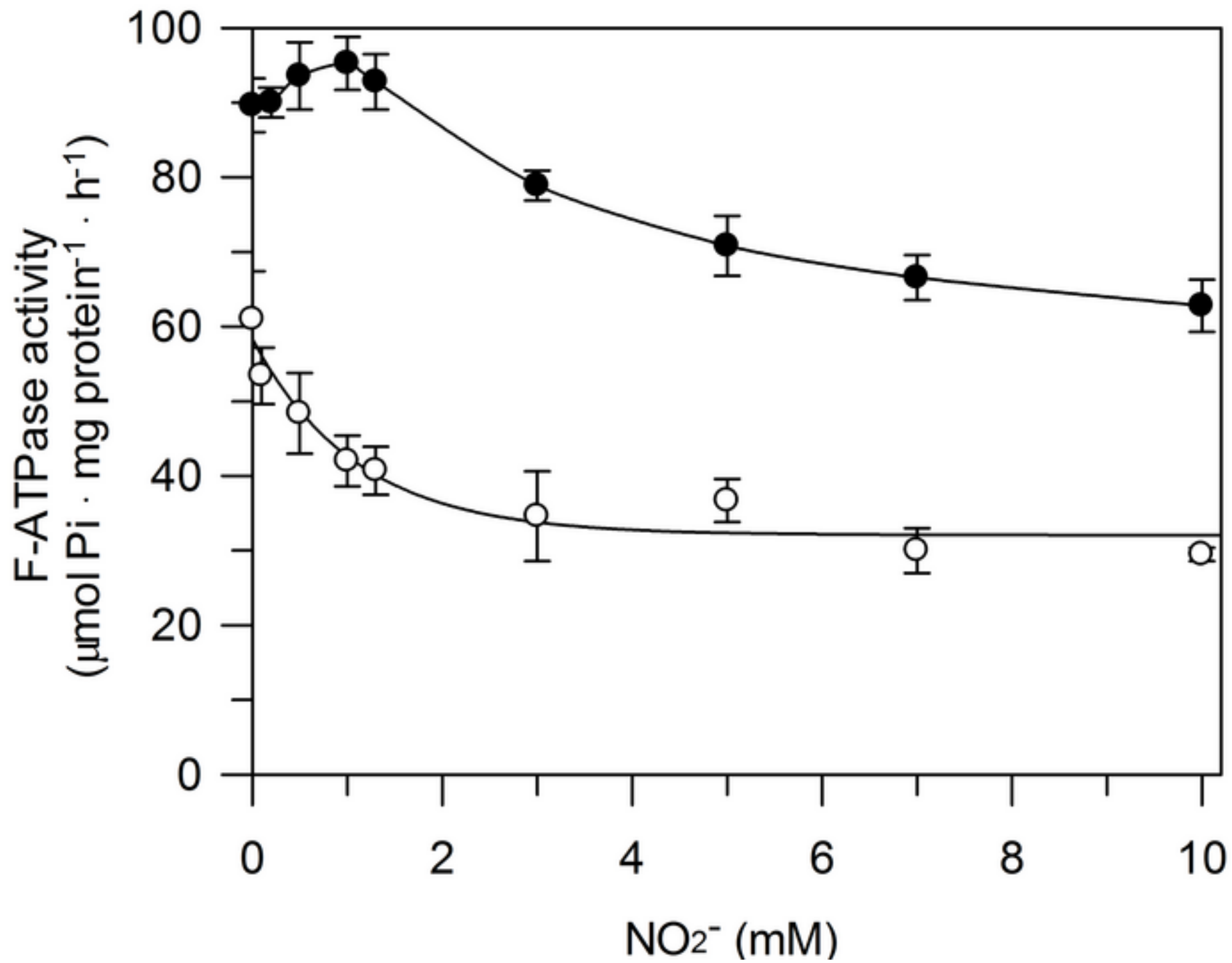


Figure 4

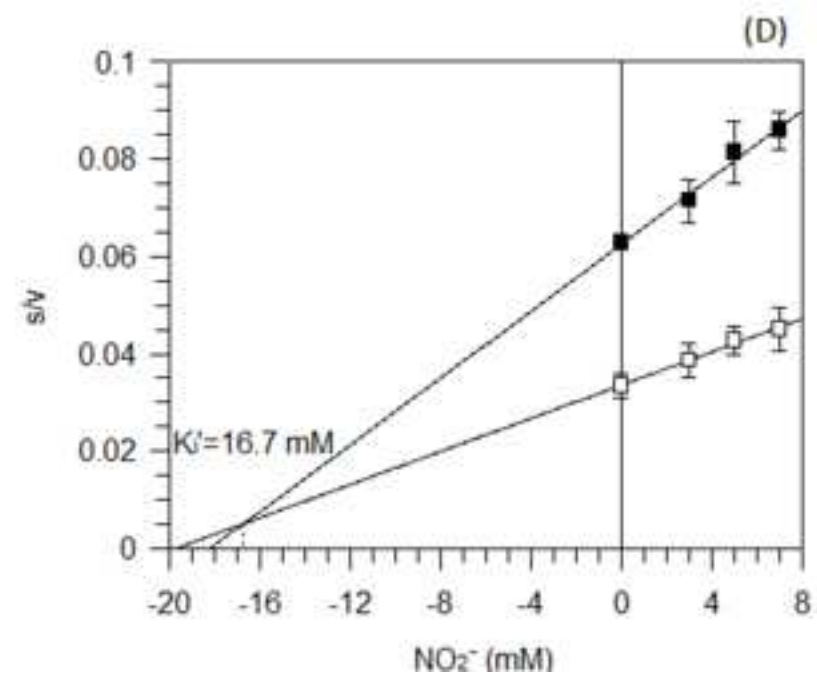
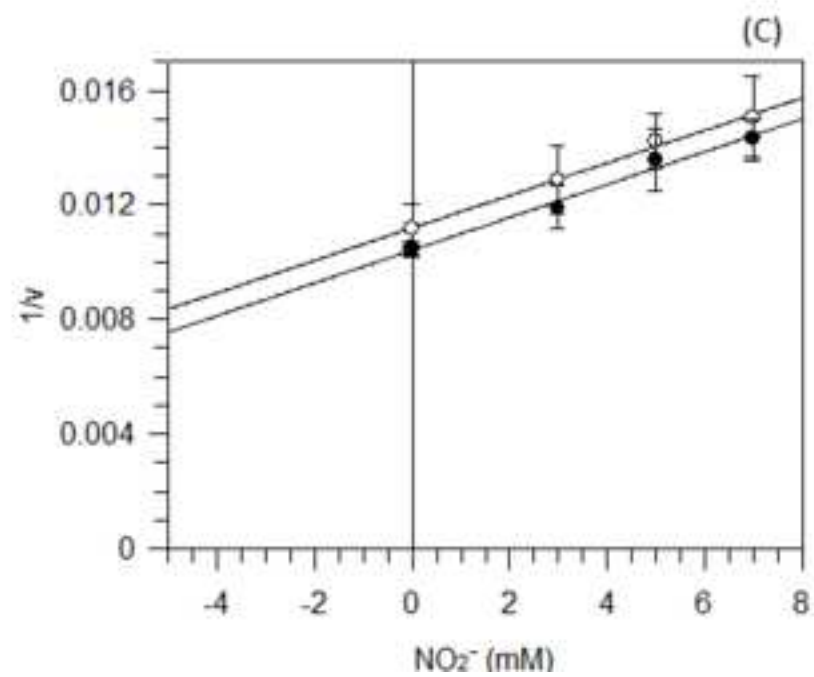
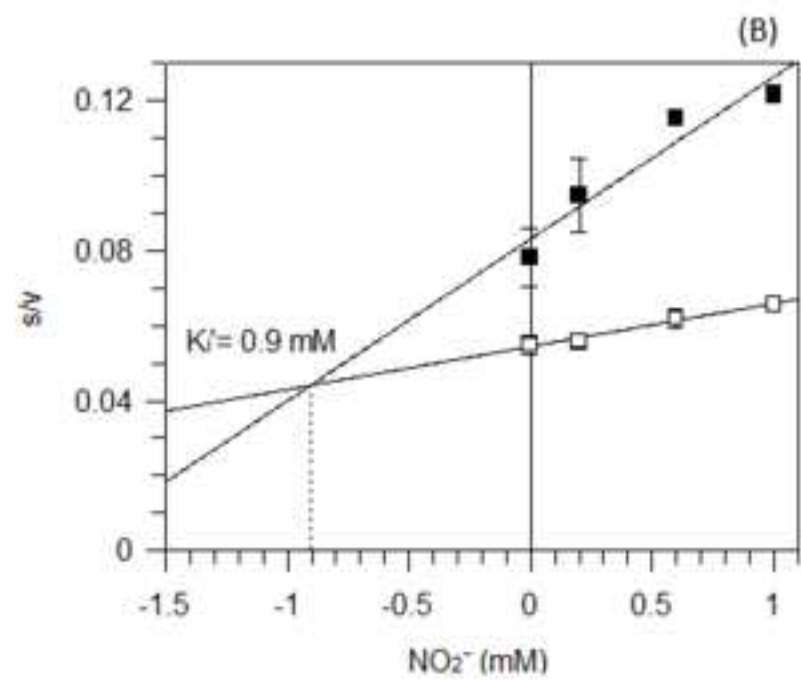
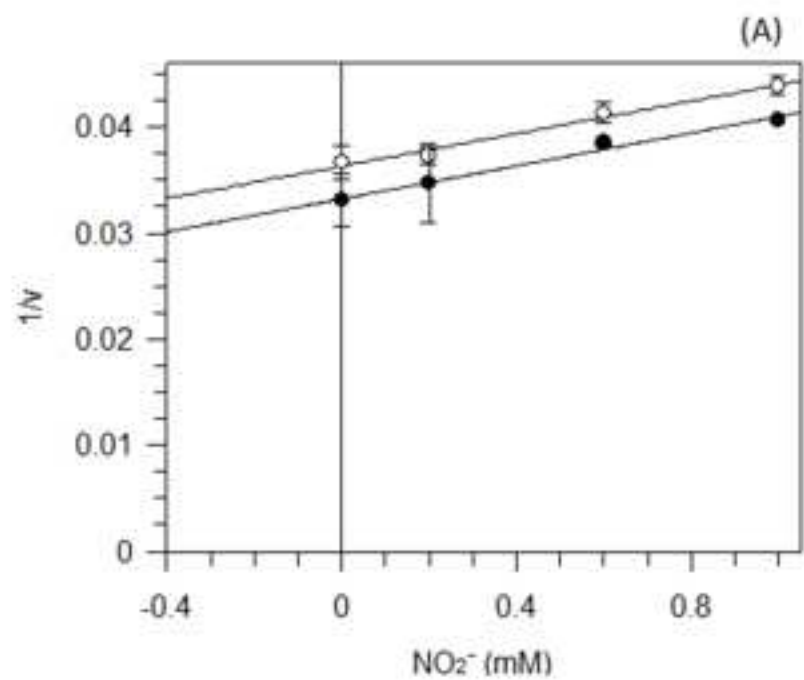


Figure 5

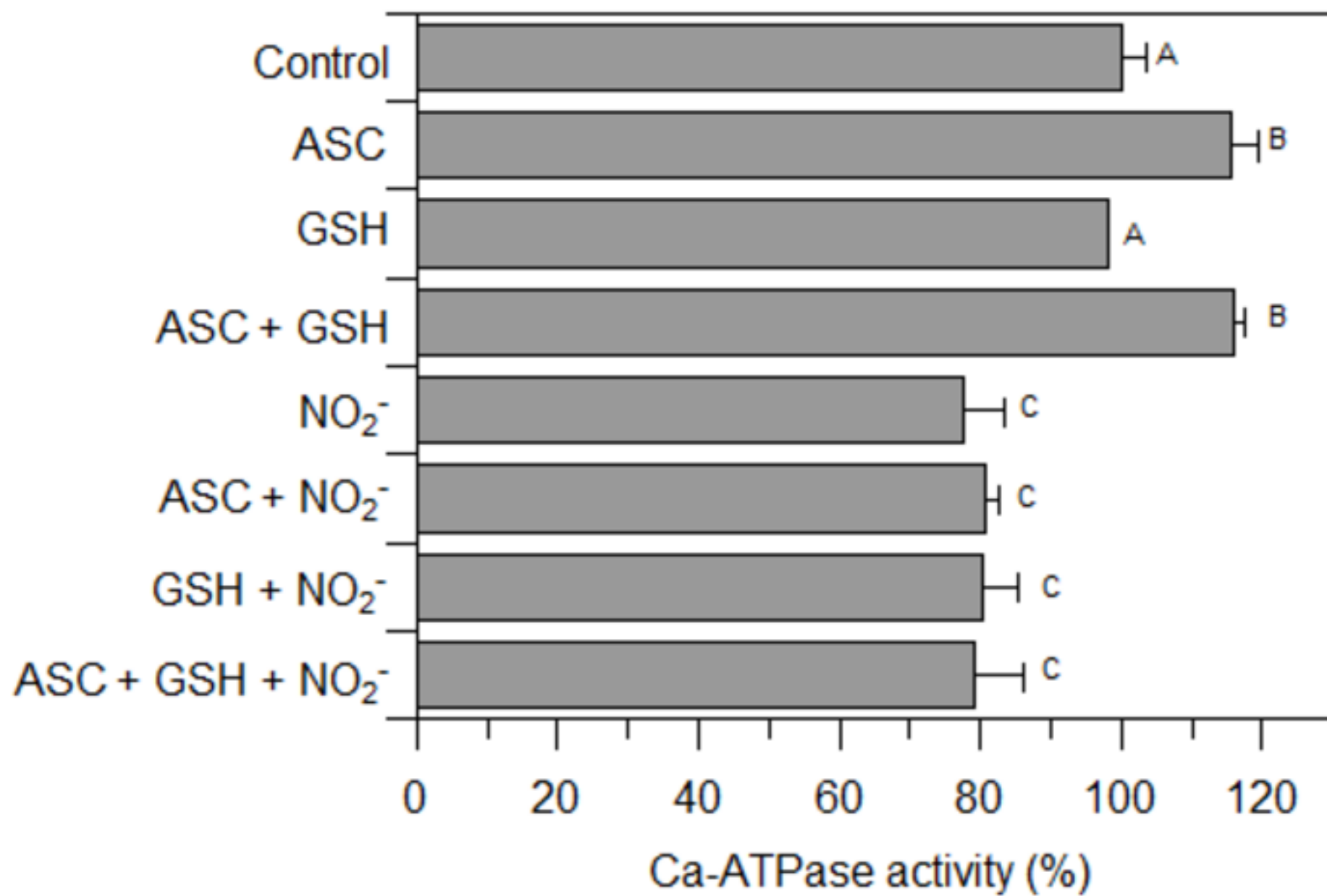


Figure 6

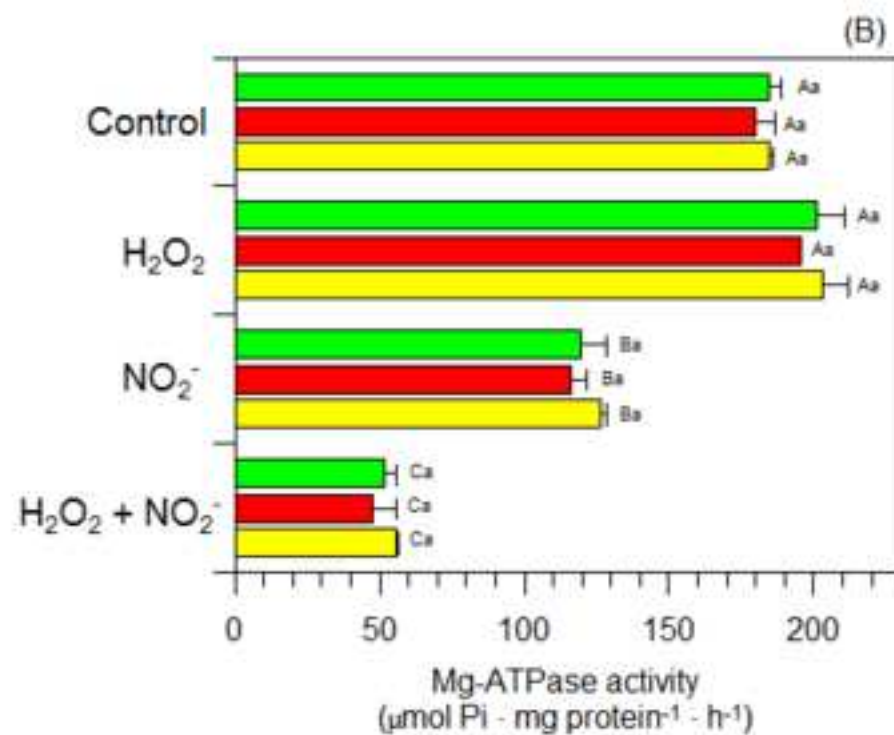
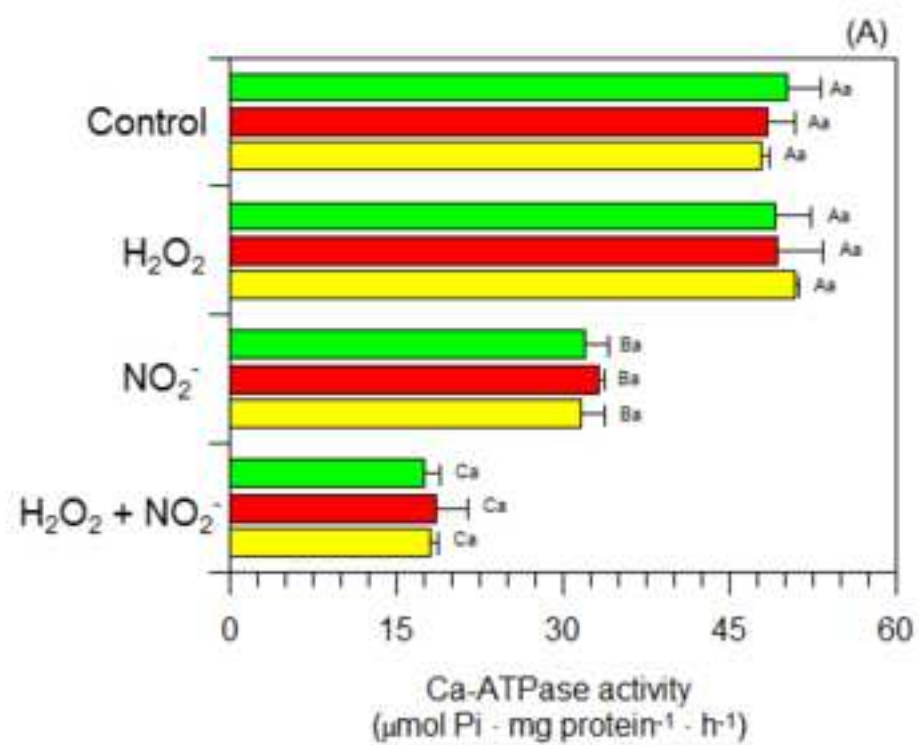


Figure 7

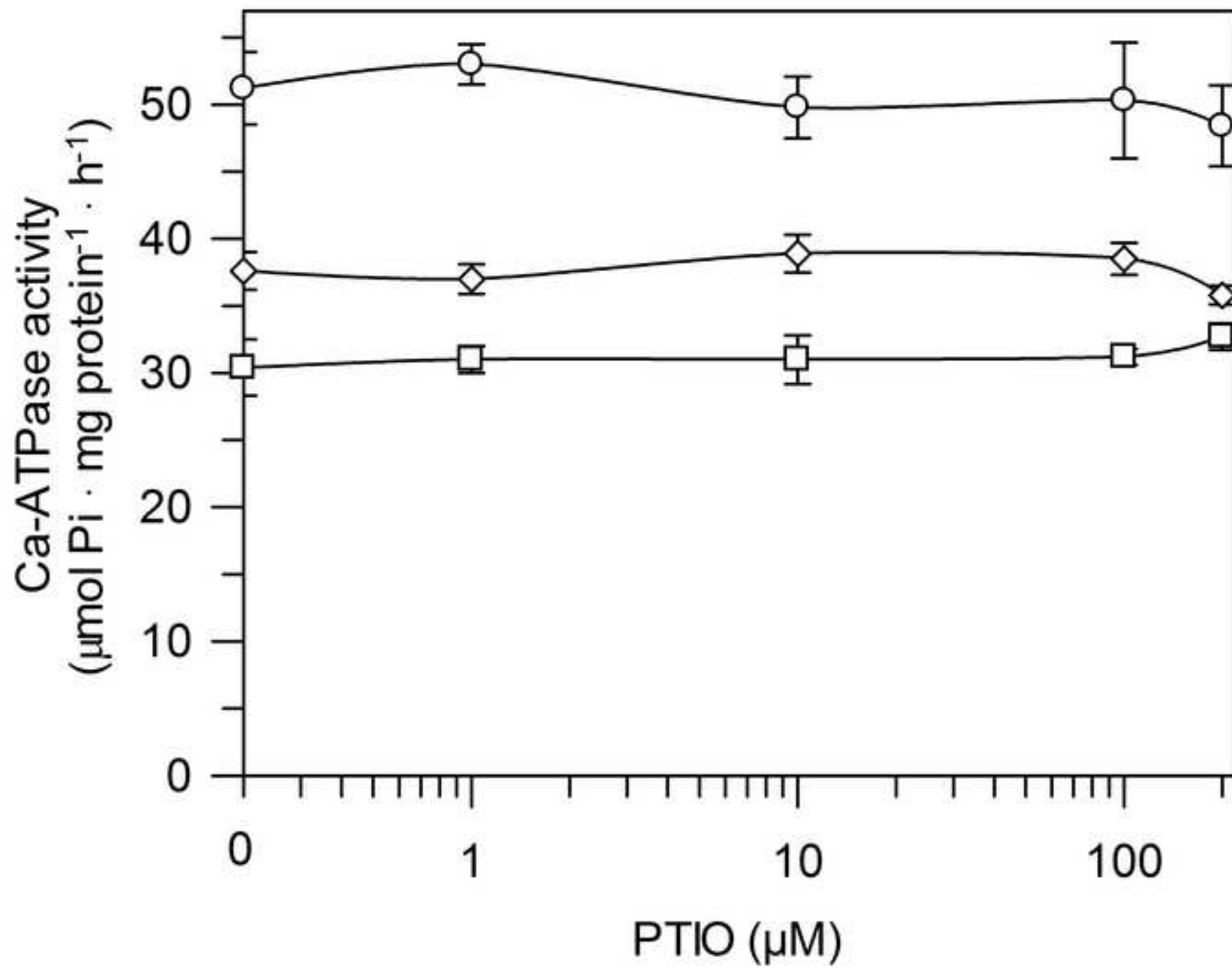


Figure 8

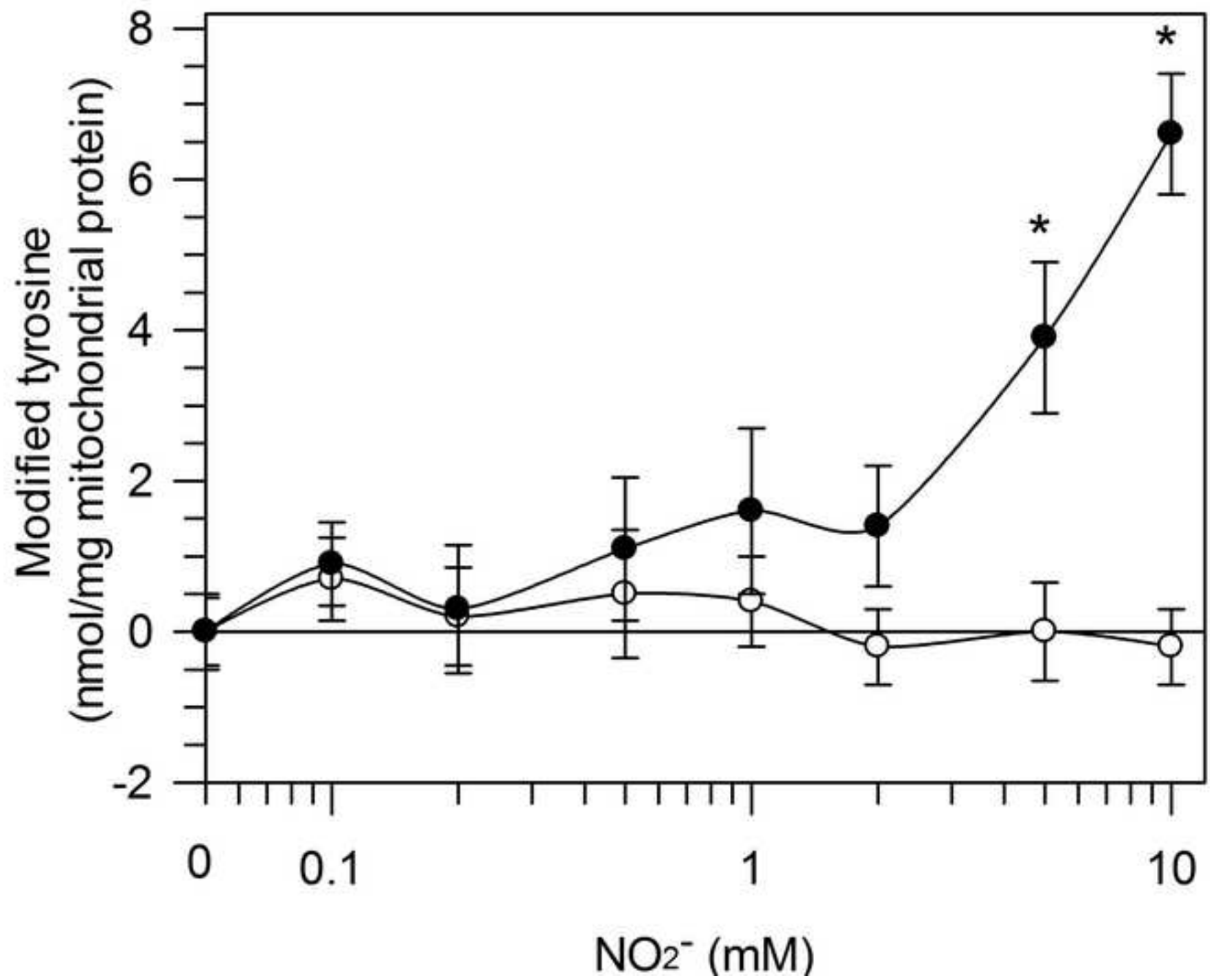


Figure 9

